Fluctuations at the self-organized critical state

Hans-Henrik Stølum
Department of Earth Sciences, Cambridge University, Downing Street, Cambridge CB2 3EQ, United Kingdom
(Received 22 July 1997)

Avalanche dynamics is defined as coupled internal motion at two separate time scales. The state parameter $S(t)$ measures the amount of tension or potential energy stored in the system. Fluctuations of $S(t)=F_d^{\uparrow}-F_a^{\downarrow}$ are caused by the action F_d on S of the driving force, giving rise to slow, continuous motion, and the antagonistic action F_a of a relaxation force causing rapid, discrete events (avalanches). The arrows indicate the directions of the forces (increase or decrease). A state parameter may be chosen such that both forces act as repellers in state space. Self-organized criticality (SOC) emerges when F_a is an internal force that exists if, and only if, F_d is present. When this contingency condition is fulfilled, the two antagonistic forces trap the system trajectory inside a SOC attractor, which is a state-space region of overlapping basins for the two types of motion. The conclusions are based primarily on the case of river meandering dynamics, described in the paper. [S1063-651X(97)07611-3]

PACS number(s): 64.60.Lx, 05.40.+j

I. AVALANCHE DYNAMICS

Avalanche or cascade dynamics arises in systems of matter that allow internal motion at more than one spatial and temporal scale (Fig. 1). Give a time scale with infinitesimal resolution dt and define two nonoverlapping sets of motion dS/dt (microscopic) and $\Delta S/dt$ (macroscopic) such that dS/dt is continuous and $\Delta S/dt$ consists of discontinuous events (avalanches, cascades), each occurring over time spans Δt_a that are either instantaneous or time extended ($\Delta t_a \geqslant dt$). Define avalanche dynamics such that the two sets of motion interact; macroscopic dynamics emerge as a consequence of microscopic change, which sporadically and locally brings the system into an unstable, critical state by exceeding geometric or force balance thresholds of stability. In this state both forms of motion become possible, and as the likelihood of each form of motion becomes equal, the system may flick from one to the other at any infinitesimally small perturbation. This unleashes a macroscopic event of local relaxation. The microscopic change is spatially global and temporally infinite, while the macroscopic motion is spatially local, always confined to regions smaller than the scale of the system, and temporally finite, contained in discrete events.

Self-organized criticality (SOC) refers to a tendency of dissipative, dynamical systems to become self-organized by avalanche dynamics (discrete events clustered in time and space) into a critical state that is independent of initial conditions. The critical state combines global stability of the system (robustness and stationary fluctuations) with local instability [1]. Avalanche dynamics also gives rise to fractal (scale-invariant or -covariant) structures in time and space [1,2]. The behavior of SOC systems is summarized in Fig. 2.

II. COMPARISON OF THE MEANDERING RIVER AND THE GRAINPILE AS DYNAMICAL SYSTEMS

Avalanche dynamics is caused by a set of instabilities. An *instability* means that properties of the system accelerate away from a given previous state when the system is perturbed (sensitive dependence on initial conditions). Conversely, a stable system will return to its previous state after perturbation. When not expressed, instabilities are present as intrinsic, potential, or possible forces.

Four instabilities arise in SOC grainpiles (the simplest case consists of even-shaped and -sized dry, cohesionless grains with high surface friction [3]): (i) Grain locking (local friction) forces vertical buildup (stacking) rather than horizontal spreading, (ii) rolling of surface grains at the angle of repose ($S=S_c$), (iii) rupture of densely stacked (locked) domains of grains near the surface, and (iv) sliding of ruptured domains and single grains. The first is a local geometrical instability; the others occur when a gravity or friction threshold is exceeded for surface grains and locked grain domains.

In the case of free river meandering, six boundary conditions appear to be necessary and sufficient for the system to exist [4]. When the six conditions are present, five instabilities will arise: (i) turbulence instability causing coherent flow structures, which lead to incipient channel cross-section asymmetry locally in straight and weakly curving channel reaches [5]; (ii) channel cross-section asymmetry–flow feedback in a straight or curved channel [6]; (iii) channel bend–flow instability causing asymmetrical lateral erosion [6]; (iv) closed loop instability causing river segments to be cut off when the river curves enough to meet itself [7]; and (v) neck instability causing regression of neck shape after cutoff (Sec. V). The first is an instability of the fluid motion; the others are instabilities of channel geometry [4].

For any SOC system, a set of instabilities generates *two opposing forces* that act on and determine S. For meandering rivers, instabilities (i)–(iii) increase S, while instabilities (iv) and (v) decrease S [7]. For grainpiles, measured by slope angle, instability (i) increases S, while instabilities (ii)–(iv) decrease S.

III. RIVER MEANDERING REPRESENTED AS A DYNAMICAL SYSTEM

The conclusions of this paper are largely based on the SOC dynamics of meandering motion [7]. This section pro-

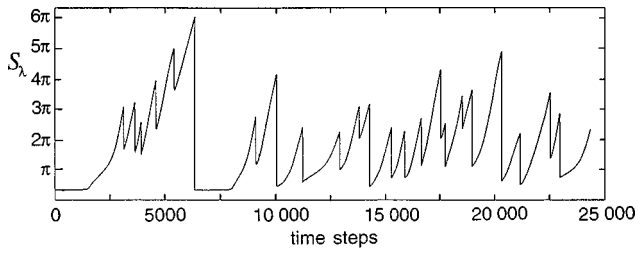

FIG. 1. Fluctuations of wavelength sinuosity S_λ from simulated free meandering river. Sinuosity is the dimensionless parameter $S=L/l$, where L is the length of the river along its course between two points and l is the shortest length between the same points. The quantitites L and l are measured in units of river width. Wavelength sinuosity is measured over a single wavelength of river meandering (Fig. 9). The mean value is $\overline{S_\lambda}=5.85\pm3.87$, close to the Kinoshita S_λ of 2π, which is the boundary point between the avalanche-generating repeller and the SOC strange attractor [cf. Figs. 7 and 10(a)].

vides a detailed description of the meandering model used. River meandering migration is a consequence of erosion at the outer bank of a river bend and deposition at the inner bank [8]. If there is no net erosion or deposition (i.e., a steady state in terms of sediment supplied to and lost from a river reach) then the average cross-section area of the whole reach will remain constant in time. This condition is common in meandering rivers, suggesting that this steady-state condition is caused largely by the negative feedback effect of momentum conservation. Most bedload material eroded at an outer bank will be deposited on the next inner bank (point bar) downstream. It is therefore sufficient to describe the migration of a meandering river in terms of the erosion process at the outer banks.

Figure 3 shows the coordinate system used in the following. The rate of erosion ζ at a channel bank is a function of the near-bank depth-averaged downstream velocity u_{sb}:

$$\zeta=\zeta(u_{sb}). \tag{1}$$

The near-bank velocity can be given as the sum of the cross-sectional average flow velocity u_{s0} and the increment near the river bank:

$$\zeta(u_{sb})=\zeta(u_{s0}+\tilde{u}_{sb}). \tag{2}$$

Since the cross-sectional area is approximately constant, u_{s0} will be almost constant along the river at any given time, but varies slowly in space around a reach-averaged velocity U, which fluctuates in time with sinuosity as the river meanders [Eq. (7)]. The increment $\tilde{u}_{sb}$ depends on both s and time. If $\tilde{u}_{sb}$ is small compared to u_{s0}, Eq. (2) can be approximated by the Taylor expansion

$$\zeta(u_{sb})=\zeta(u_{s0})+\left.\frac{d\zeta}{du_{sb}}\right|_{u_{sb}=u_{s0}}\tilde{u}_{sb}=\zeta(u_{s0})+E(u_{s0})\tilde{u}_{sb}, \tag{3}$$

where the erosion function $E(u_{s0})$ may depend on the average flow velocity u_{s0} as well as the resistance to erosion of the bank material. If the variation of u_{s0} is sufficiently small, the erosion function can be approximated by an erosion coefficient E that is independent of u_{s0}. When the thalweg (path of highest flow rate in successive downstream cross sections) is centered in the channel, no erosion takes place that contributes to the meandering motion (erosion may change the cross-sectional channel shape, but will not induce asymmetry). In this state $\zeta(u_{sb})=\zeta(u_{s0})=0$. Hence ζ can be approximated by

$$\zeta=E\tilde{u}_{sb}. \tag{4}$$

This linear relationship between bank erosion rate and the near-bank velocity fluctuation has been confirmed by empirical measurements [9]. At the same time, $\tilde{u}_{sb}$ will adjust instantaneously relative to the rate of channel migration; this feedback effect is one of the instabilities that drive the meandering motion [instability (ii)].

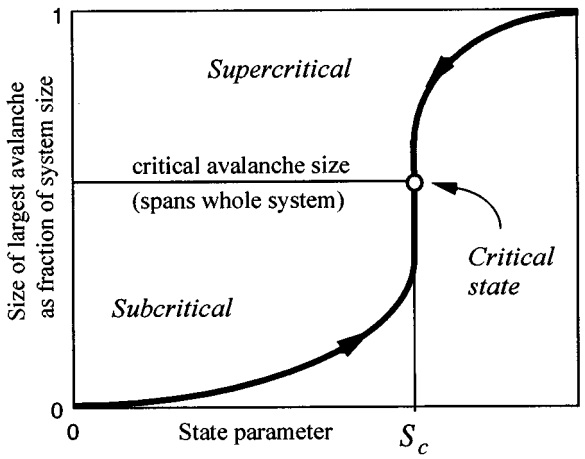

FIG. 2. SOC dynamics. The smallest value of S that allows avalanches to span the whole system is the critical state. The system is *globally independent* of initial conditions (robust, i.e., resilient to perturbations) in the sense that it will go to the critical state from any starting point. At the same time it is *locally sensitive* to initial conditions in the sense that any change of the initial conditions will cause a divergence of local trajectories within SOC.

Ikeda, Parker, and Sawai [8] obtained solutions to the depth-averaged St. Venant equation for shallow water flow

$$U_0=\left(\frac{gQI_0}{2bC_f}\right)^{1/3}, \tag{5}$$

$$H_0=\frac{Q}{2bU_0} \tag{6}$$

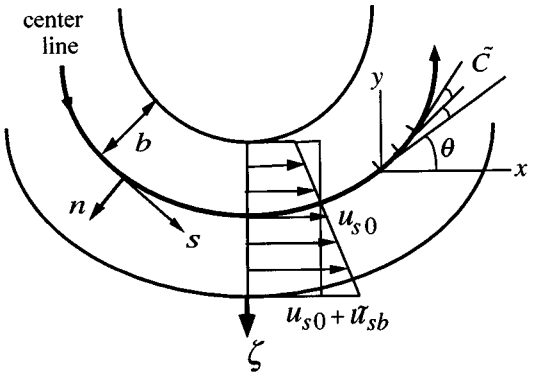

FIG. 3. Notation and variables.

by solving the St. Venant equation for uniform flow along a straight channel with the same overall slope as the meandering river, using a small-perturbation approach to linearize the governing equations in the region around the uniform flow solutions. U_0 is the steady-state flow velocity of the straight channel and H_0 the average depth. Q is the total volumetric flow in the channel (discharge) and I_0 is the slope of the flood plain. For a sinuous channel, the slope is smaller than I_0 and so the reach-averaged flow velocity is lower. Define sinuosity as

$$S=\frac{L}{l}=\frac{I_0}{I},$$

where L is the length of the meandering channel reach, l is the length of a straight channel reach between the same end points, and I is the slope of the meandering channel. This yields the reach-averaged velocity of the meandering channel as

$$U=U_0 S^{-1/3}. \tag{7}$$

Ikeda, Parker, and Sawai [8] found that St. Venant's equation yields an expression for flow in a meander bend that allows calculation of the near-bank velocity increment that determines ζ:

$$u_{s0}\frac{\partial \tilde{u}_{sb}}{\partial s}+2\frac{u_{s0}}{h_0}C_f\tilde{u}_{sb} =b\left[-u_{s0}^2\frac{\partial \tilde{\omega}}{\partial s}+C_f\tilde{\omega}\frac{u_{s0}^2}{h_0}(F^2+A+A_s-1)\right], \tag{8}$$

where the partial differential form represents the fact that $\tilde{u}_{sb}$ and $\tilde{\omega}$ are functions of both s and time. Hence the equation describes change occurring in s at any instant in time. In Eq. (8), h_0 is the average depth of the channel, b is the half-width of the river, $\tilde{\omega}$ is the local curvature of the river center line (Fig. 3 shows two measures of this parameter, $\tilde{c}$ and θ), $F=u_{s0}/\sqrt{gh_0}$ is the Froude number, g is acceleration due to gravity, A is a proportionality constant in Eq. (12), and A_s is a constant accounting for the momentum redistribution due to the secondary flow in bends [10]. This helicoidal vortex movement is the largest-scale coherent structure of turbulent flow in meander bends [11].

The friction coefficient C_f used in Eq. (8) is defined by the relationship

$$\boldsymbol{\tau}_s=\mathbf{u}(\mathbf{u}\cdot\mathbf{v})^{1/2}C_f, \tag{9}$$

where $\boldsymbol{\tau}_s$ is the shear stress on the river bed in the downstream direction and $\mathbf{u}$ and $\mathbf{v}$ are the depth-averaged downstream and transversal flow velocities in the channel [12]. The friction coefficient depends on the bed form structure and material on the river bed, but tends to vary within a relatively narrow range in meandering rivers. It may therefore be approximated by a constant, representing the average boundary friction.

Although $\tilde{u}_{sb}$ and $\tilde{\omega}$ are functions of both s and time, $\tilde{u}_{sb}$ is assumed to adjust instantaneously relative to the rate of channel migration. Hence, at any instant in time, Eq. (8) can be treated as an ordinary differential equation and may be solved using an integrating factor [13]. At a sufficient distance from $s=0$ the solution takes the form

$$\tilde{u}_{sb}=-bu_{s0}\tilde{\omega}+\frac{bC_fu_{s0}}{h_0}[F^2+(A+A_s+1)] \times\int_0^{s'_{\max}}\exp(-2C_fs'/h_0)\tilde{\omega}(s-s')ds'. \tag{10}$$

Hence $\tilde{u}_{sb}$ is determined by the local curvature, with a correction arising from nearby upstream points, in the simulator corresponding to a distance $s-s'_{\max}$ (short-distance memory effect).

The axis n, normal to the downstream direction at any point along the channel center line, is always taken as increasing toward the left bank when looking downstream (Fig. 3). The value of $\tilde{u}_{sb}$ obtained from either Eq. (8) or (10) refers to the left bank, with the velocity increment at the right bank then having the value $-\tilde{u}_{sb}$. The curvature $\tilde{\omega}$ is positive or negative, depending on whether the river is curving clockwise or counterclockwise. The value of $\tilde{u}_{sb}$ can therefore be positive or negative, depending on whether it is the left- or the right-hand-side of the river that is being eroded.

Lateral meandering migration of the channel increases local curvature, giving a monotonically increasing relationship $\tilde{\omega}=f(\zeta)$, which leads to an instability in the form of positive feedback. However, the correction term for local geometry in Eq. (10) (determined by bend entrance conditions at inflection points) complicates the nature of the instability by introducing competing interactions between neighboring bends. This leads to frequent local and temporary quenching of instability (ii), which nonetheless is fundamentally a positive feedback interaction.

Equation (8) is a depth-averaged representation of the flow conditions. It therefore does not describe the cross-sectional asymmetry of the channel shape due to point bars and alternate bars, which gives rise to another essential instability in the meandering process [instability (iii)]. Ikeda, Parker, and Sawai [8] represented the coupling between flow field and the cross-sectional bed topography linearly:

$$\tilde{\eta}(n)=Ah_0\tilde{\omega}n. \tag{11}$$

As before, h_0 is the average depth of the channel, $\tilde{\eta}(n)$ is the river bed elevation relative to some horizontal level, and n is the coordinate in the direction perpendicular to the center line (Fig. 3). A is a positive constant (the ''scour factor''). Equation (11) agrees with the experimental data of [14].

Although this linear relationship gives a first-order representation of instability (iii), it is too simple to accurately describe the flow field-channel cross-section asymmetry feedback. Planforms generated from Eq. (8) have been compared to the lateral migration of rivers [10]. A reasonable fit was found only if unrealistic values were assigned to the parameters. The effect of these deviations from the natural parameter ranges was to push the distribution of high flow velocity further toward the outer bank of the river. The problem is that the real interaction depends not only on curvature but also on upstream flow conditions (the entrance condi-

tions into each bend). This local memory effect causes overdeepening in parts of the bends compared to the topography predicted by Eq. (11).

Johannesson and Parker [10] achieved a more exact channel deformation response to variation in the flow field by representing the interaction as three sediment transport relationships, assuming a slowly varying erodible bed: sediment mass conservation

$$\frac{\partial \eta}{\partial t}+\frac{Q_0}{1+nb\tilde{\omega}}\left\{\frac{\partial q_s}{\partial s}+\frac{\partial[(1+nb\tilde{\omega})q_n]}{\partial n}\right\}=0, \qquad (12)$$

the downstream sediment transport relationship

$$q_s=q_{s0}\left[\frac{u_{s0}}{U}\right]^M, \qquad (13)$$

and the transverse sediment transport relationship

$$\frac{q_n}{q_s}=\frac{v_{n0}}{u_{s0}}+\frac{\nu_0}{T_0 u_{s0}}-\beta\frac{h_0}{b}\frac{\partial \eta}{\partial n}. \qquad (14)$$

In Eqs. (12)–(14), v_{n0} is the depth-averaged transversal flow velocity, q_s is the downstream volumetric sediment transport rate, q_n is the transversal volumetric sediment transport rate, ν_0 is a term describing the secondary flow in bends, T_0 describes the vertical flow velocity profile (logarithmic), and U is the reach average of the flow velocity u_{s0}. Q_0 is a function relating the total sediment discharge in the reach to U. The constant β expresses a transverse force balance relation on a sediment particle moving along an inclined bed [15,10]. Equation (13) introduces variation of u_{s0} into the model as a consequence of slow variation in the cross-sectional area caused by sediment transport. This relationship is part of a negative feedback interaction that causes a tendency to an approximately constant cross-sectional area. The ratio u_{s0}/U is therefore close to unity and Eq. (13) is roughly linear.

Meandering motion causes the river to occasionally meet itself, which invariably result in cutoff of a loop-shaped segment of the river [instability (iv)]. This neck cutoff phenomenon was studied by Parker and Andrews [13]. Curvature $\tilde{\omega}(s,t)$ at a given time and position s on the center line, where s is the distance along the center line from an original point (also on the center line), may be given as

$$\tilde{\omega}=-\frac{\partial \theta}{\partial s}, \qquad (15)$$

where θ is the angle of local channel center line deflection measured relative to an external frame of reference (x,y) (Fig. 3). Many other measures of curvature are possible; however, it was found by Sun, Meakin, and Jøssang [12] that the actual measure used does not affect the simulation outcome. Using definition (15) and Eq. (8), Parker, Sawai, and Ikeda [16] found that

$$\frac{u_{s0}}{U}\frac{d^2\theta}{ds^2}+\left[c\,\cos\theta-AC_f\left(\frac{u_{s0}}{U}\right)^2\right]\frac{d\theta}{ds}+2C_f\frac{u_{s0}}{U}\,c\,\sin\theta=0, \qquad (16)$$

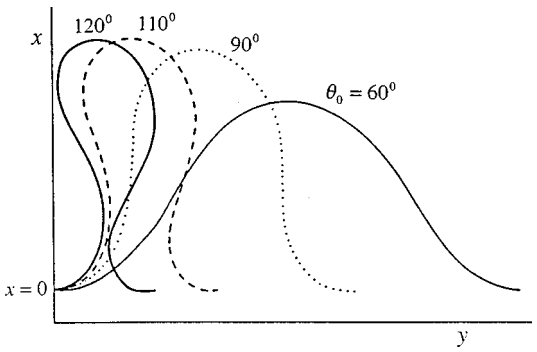

FIG. 4. Solutions of permanent form of Eq. (17). Flow is from left to right. From [13].

where $c=\tilde{c}/U$ and $\tilde{c}$ is the downstream migration rate of perturbations.

From Eq. (16), Parker, Sawai, and Ikeda [16] obtained an analytical solution, termed the Kinoshita curve. Let λ_a denote the arc meander wavelength and $\kappa=2\pi H_0/\lambda_a$ denote the dimensionless arc wave number. θ_0 is an angle amplitude taken to be small,

$$\theta=\theta_0\sin\phi+\theta_0^3\left[\frac{1}{192}\sin 3\phi+\frac{\sqrt{2A}}{128}\cos 3\phi\right], \qquad (17)$$

where $\phi=\kappa s$. The family of solutions given by Eq. (17) are plotted in Fig. 4 for $A=2.89$, found to be a characteristic value by empirical measurements [8]. Parker and Andrews [13] demonstrated that the solution (17) is not stable, i.e., bends will grow to cutoff, and the final meandering dynamics will depend strongly on the cutoff process.

Cutoff generates a particular type of bend, the neck shape (Fig. 5). The model predicts that bends formed by cutoffs will recede by deposition on the outside and erosion on the inside of the bend [instability (v)]. This is caused in the model by the migration derived from Eq. (8) or (10), where erosion of the inner bank is due to a combination of the entrance condition into the bend, represented explicitly in Eq. (10) as the term for local upstream effect, and the particular geometry of the bend itself. Necks subside until local curvature falls below a threshold due to change of shape.

Give the amount of time required for a bend to increase or decrease in amplitude from an initial value of θ_0 to a final value of θ_F as $\Delta\tau_r$. Parker and Andrews [13] found this interval as

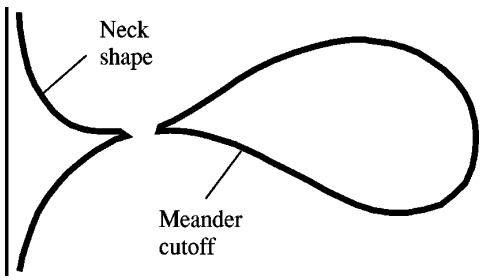

FIG. 5. Local river neck shape at t_i (after cutoff) has the same sinuosity as a semicircle; $S_N=\pi/2$.

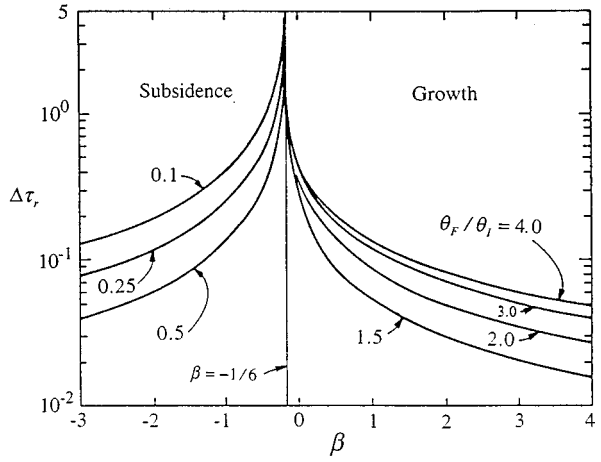

FIG. 6. Time lag of meander angle amplitude change [Eq. (18)] as a function of β [Eq. (19)] for different ratios of final to initial angle amplitude θ. From [13].

$$\Delta\tau_r = \frac{1}{12\beta}\ln\left[\frac{(\theta_F/\theta_0)^2(6\beta+1)}{6\theta+(\theta_F/\theta_0)^2}\right], \tag{18}$$

where

$$\beta = \frac{k_c - k}{k_c\theta_0^2}; \tag{19}$$

$k_c = (2A)^{1/2}C_f$ and $k = 2\pi H_0/\lambda$ are wave numbers. Bends are stable when $\beta = -\frac{1}{6}$. Subsidence occurs for smaller values and growth of bends when values are larger (Fig. 6).

IV. THE STATE PARAMETER OF SELF-ORGANIZED CRITICAL SYSTEMS

The state parameter $S(t)$ of a dynamical system measures the state of the whole system such that dS/dt and $\Delta S/dt$ represent all microscopic and macroscopic motion within the system. The critical state corresponds exactly to one and only one value of S. Avalanche dynamics may be represented in state space as a trajectory of change in $S(t)$ (Fig. 7).

Several measures may act as the state parameter for a given system. For a meandering river the simplest possible state parameter is the sinuosity $S = L/l$, where L is the size of the system (length of the river along its course between two points) and l its dimensional span (the straight line length between the same two points). $1 \leqslant S \leqslant \infty$ and the critical state is given by $S = \pi$. A more complex possible state parameter is the fractal (similarity) dimension. For a two-dimensional grainpile, the simplest state parameter is the whole slope angle between the apex and the edge of the pile. Alternatively, a sinuosity equivalent measure may be used such that L is the detailed length of the slope and l is the straight-line distance from apex to the edge of the pile. It is not important which measure is used since any state parameter by definition will record the fluctuations of the system. I shall assume in the following that S refers to sinuosity when the system is a river and to a whole slope angle when it is a grainpile.

Fluctuations of the state parameter $S(t)$ can be expressed

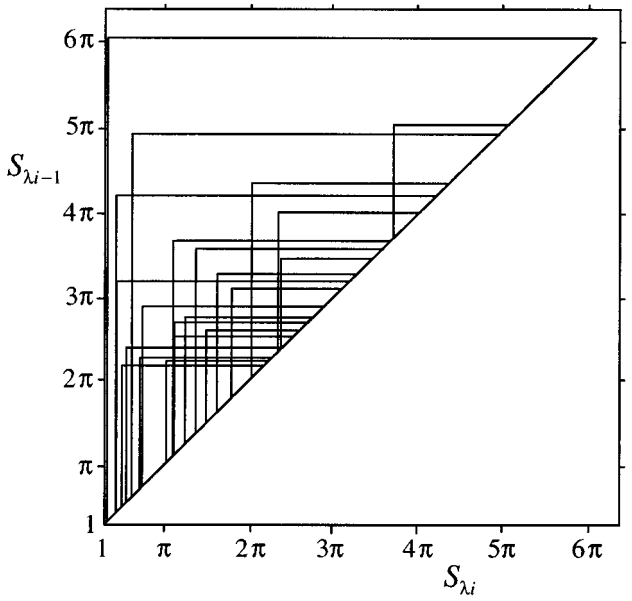

FIG. 7. Avalanche dynamics of free river meandering represented as a trajectory of wavelength sinuosity in state space, corresponding to the time-series interval in Fig. 1.

in terms of two forces or force complexes with opposite direction, one increasing and one decreasing S. One force $F_d = f(ds/dt)$ is caused by the slow, continuous driving process of the system; the other $F_a = f(\Delta s/dt)$ is caused by discrete events, but may also involve secondary, continuous changes:

$$S(t) = F_d(v,t) - F_a(v,s,t),$$

where $s = (x_1, x_2, x_3)$ is space, t is time, and v is the rate of driving for the system in question. F_d is evenly distributed in space and therefore only a function of time and rate of driving. F_a is localized in space and a function of local spatial properties of the system and is therefore also a function of space. Hence

$$S(t) = F_d^{\uparrow}(v,t) - F_a^{\downarrow}(v,s,t). \tag{20}$$

Which of the forces increases S, $F^{\uparrow}$, and which decreases it, $F^{\downarrow}$, depends on how S is defined to measure the state of the system and both $S(t) = F_d^{\uparrow} - F_a^{\downarrow} = F_a^{\downarrow} - F_d^{\uparrow}$ carry exactly the same information content. In any case, the action of F_d on S increases the potential energy in the system and F_a acts to convert potential energy into kinetic energy and heat.

V. DETERMINISTIC REPRESENTATION OF FLUCTUATIONS AT THE CRITICAL STATE

With reference to Eq. (20), let us define the state parameter value before and after a single avalanche ΔS_i as S_i^{high} and S_i^{low}, where i refers to the time t_i of occurrence of the avalanche. The driving force is constant and therefore has a linear, cumulative effect on sinuosity:

$$F_d^{\uparrow} = S_{i-1}^{\text{low}} + vt, \tag{21}$$

where $i-1$ refers to the last occurring avalanche, $i-1 < t < i$. In the case of river meandering, sin α is the gradient of

the plain on which the river flows. This is a measure of the strength of the driving force and therefore determines how fast $F_d^{\uparrow}$ increases S; thus $v=b\ \sin Z\alpha$, where b is a positive constant. The action of F_a is given by

$$F_a^{\downarrow}=F_a^{\uparrow}=f_D(v,s,t)+f_C(t)=I(\Delta t_i)\Delta S_i+f_C(t), \quad (22)$$

where $f_D(v,s,t)$ is a discrete (avalanche) component and $f_C(t)$ any secondary continuous component caused by the avalanche process.

Each avalanche occurs in a brief, finite time interval $\Delta t_a=t_j-t_i$, $\Delta t_a \ll \Delta t$, where Δt is the time interval between successive avalanches; hence avalanches are discrete events and avalanche dynamics is a discontinuous process (in the case of river meandering, each avalanche takes the form of a cutoff event that is infinitesimal in duration $\Delta t_a=dt$, but on grainpiles avalanches occur during finite time intervals). $\Delta S_i=\Delta S_{i,n}$ represents the avalanche occurring during time $\Delta t_{a,n}=t_{j,n}-t_{i,n}$, where the subscript n is the nth successive avalanche. Given a time interval between two successive avalanches $\Delta t_i=\Delta t_{i,n}=t_{i,n}-t_{j,n-1}$, then we may define an indicator function $I(\Delta t_i)=\{0,1\}$, 0 if ΔS_i is a future event and 1 when $t=t_i$:

$$I(\Delta t_i)=\begin{cases}0, & t_{i,n-1}<t<t_{i,n}\\ 1, & t=t_i.\end{cases}$$

This requires the time interval between successive avalanches Δt_i to be known while the present time t is still inside Δt_i (however, this knowledge is only required just before $t=t_i$). The necessary information comes from details of the spatially extended dynamics of the system, as does information about ΔS.

For any general SOC system, temporal fluctuations around the critical state occur according to

$$\begin{aligned}S(t)&=F_d^{\uparrow}(v,t)-F_a^{\downarrow}(v,s,t)\\ &=\{S_{i-1}^{\text{low}}+vt\}-\{I(\Delta t_i)\Delta S_i+f_C(t)\},\end{aligned} \quad (23)$$

where the term $f_C(t)$ may or may not be present (it is absent, for instance, in SOC grainpiles without creep relaxation after avalanches). The directions of F_d and F_a are always opposite. In time, they are coupled only through the resetting of S by S_{i-1}^{low}, which derives from $\Delta S_{i-1}=S_{i-1}^{\text{high}}-S_{i-1}^{\text{low}}$. The physical structure of the coupling is located in the spatial domain.

For river meandering, $f_C(t)$ is a continuous element of $F_a^{\downarrow}$ due to the neck instability [instability (V)]. It reduces the increase of S immediately after avalanches, causing periods of increase to become weakly nonlinear. In SOC systems without this secondary element, a linear continuous change of the state parameter is common; cf. [7,17].

In the river meandering case, simulations show that $f_C(t)$ is an exponential decay function. Irrespective of the magnitude of ΔS_t, the neck residual (Fig. 5) may be considered to span a constant river length (for a given river width w) irrespective of the size of the cutoff loop. Within this span, the unstable shape has a local sinuosity $S_N=\pi/2$ immediately after the cutoff.

During neck relaxation, this sinuosity decays to a lower threshold $S_N\approx 1.3$ over a constant time span $\Delta t_N=t_i-t_N$. (The neck shape regresses and at the same time changes shape. The relaxation stops when the shape has been transformed back to a meander shape, i.e., a shape that allows the fastest flow path to follow the outer bank of the bend.) Assume the simplest case of constant relaxation (erosion) rate of the neck axis during the decay period. A constant rate is equivalent to an exponential decay function of the neck shape as a whole. The contribution of $f_C'(t)$ to the sinuosity of the whole system $S=L/l$ depends on the length span of the instability $N=2\pi w$ relative to the linear length of the system lw or $N/lw=2\pi/l$,

$$f_C(t)=\frac{2\pi}{l}\,\frac{\pi}{2}\,\exp\left[-\frac{1}{2}\,\frac{k(t-t_i)}{\Delta t_N}\right].$$

It seems reasonable to allow the possibility of a variable rate of local erosion (relaxation) of the neck shape $d\varepsilon_N/dt$, which is measured relative to a characteristic mean erosion rate of $d\varepsilon/dt=1$ over the same interval when the neck shape is not present. Hence

$$f_C(t)=\frac{\pi^2}{l}\,\exp\left[-\frac{1}{2}\,\frac{d\varepsilon_N}{dt}\,\frac{t-t_i}{\Delta t_N}\right].$$

For constant erosion rate $d\varepsilon_N/dt=k$. But if $d\varepsilon_N/dt$ also relaxes from a high initial value $d\varepsilon_N^{\max}/dt>1$ to the relative value characteristic of erosion due to the driving force $d\varepsilon/dt=1$, then $d\varepsilon_N/dt$ may take the form

$$\frac{d\varepsilon_N}{dt}=\frac{d\varepsilon_N^{\max}}{dt}\,\exp\left[-\frac{1}{2}\,\frac{t-t_i}{\Delta t_N}\right].$$

VI. STATE-SPACE REPRESENTATION OF SOC DYNAMICS

The temporal fluctuations of any SOC system can be represented as a trajectory in the state space spanned by S and time. $S(t)$ is only partly known, but an $S(t)$ time series from simulation of the system may be used to reconstruct the trajectory in a state space spanned by previous S vs present S (containing the time dimension implicitly) [18]. If all trajectories in a definite region of state space approach a particular limiting point set as t goes to infinity, then that point set, or fixed point, is called an *attractor*. Once at the attractor, the trajectory is not displaced. The set of initial conditions yielding such trajectories is the basin of attraction (a finite region of phase space surrounding the attractor). Another invariant set, the repeller, has the opposite effect. *Repellers* cause divergence by expelling or deflecting all trajectories into a basin of repulsion. An attractor is a *stable* fixed point in the sense that trajectories that start near it are drawn toward it. A repeller is an *unstable* fixed point in analogy with a ball rolling off the top of a hill. The top of the hill is an equilibrium point; the trajectory will not be displaced when exactly at the point, but the situation is unstable: Any infinitesimal perturbation causes the ball to roll away.

Fixed (invariant) points or point sets in state space are defined by $dS/dt=0$ [18]. For any system, a state parameter may be found such that the minimum value $S_{\min}$ is a fixed point. For example, a flat grainpile $S=0$ corresponds to an invariant point since $S_{\min}$ is unchanged by perturbations (ad-

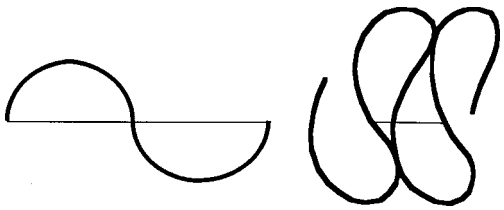

FIG. 8. Left, semicircles, $S_\lambda = \pi/2$; right, Kinoshita shape, $S_\lambda = 2\pi$.

dition of grains) on an infinite surface. A straight channel $S = 1$ is also a fixed point since differential (bend-initiating) deformations does not occur (in this geometry) if the flow is laminar [19].

A fixed point may be stable (attracting trajectories) or unstable (repelling trajectories) [18]: for $dS/dt = 0$,

$$dS^2/dt^2 < 0 \Rightarrow \text{stable (attractor)},$$

$$dS^2/dt^2 > 0 \Rightarrow \text{unstable (repeller)}.$$

To any fixed point S_0 there is a surrounding basin of attraction or repulsion

$$\{\boldsymbol{S}_A | [S_0 < (S+dS) < S] \wedge [S_0 > (S+dS) > S]\},$$

$$\{\boldsymbol{S}_R | [S_0 < S < (S+dS)] \wedge [S_0 > S > (S+dS)]\}.$$

$S_{\min}$ is always a repeller for ds/dt with $\{\boldsymbol{S}_R\}$ extending either to S_c or any value of S. The flat grainpile corresponds to an unstable fixed point since instability (i) always moves the system away from it until it reaches S_c. For meandering rivers, since instability (ii) arises spontaneously in any straight channel when flow is intermittently turbulent [5,6], $S_{\min}$ is unstable; the system will either stay on it (laminar flow) or move away from it (turbulent flow). $\{\boldsymbol{S}_R\}$ extends to any S.

Instability (iii) (cutoff events) occurs spontaneously at points of closure when the river forms a loop. The simplest (and also most common) shape of closed loops is the asymmetric Kinoshita shape, which has a wavelength sinuosity $S_\lambda = 2\pi$ (S_λ refers to the minimum value of l that allows avalanches to occur) [7] (Fig. 8). Any river segment with S_λ above this value is unstable; hence all geometries represented in the set $S_a = \{S_\lambda \geqslant 2\pi\}$ repel the macroscopic motion $\Delta s/dt$. The repelling action occurs as discontinuities of the trajectory where the system is instantaneously transferred to some point in $\{S_{\lambda R} | S_\lambda < 2\pi\}$ (Fig. 7).

Frequently in free meandering, meander bends become cumuliform, i.e., with small meanders superimposed on a larger one. Cumuliform bends tend to be broken up by the cutoff of the more rapidly growing small bends inside it and thus generate an avalanche of Kinoshita cutoffs, but they are sometimes cut off as a whole and then yield wavelength sinuosities up to approximately 6π (the largest value observed in simulations), as well as the largest cutoffs possible in the system.

The avalanche repeller S_a is indirectly caused by the action of $S_{\min}$ and therefore arises *if and only if* $S_{\min}$ is present

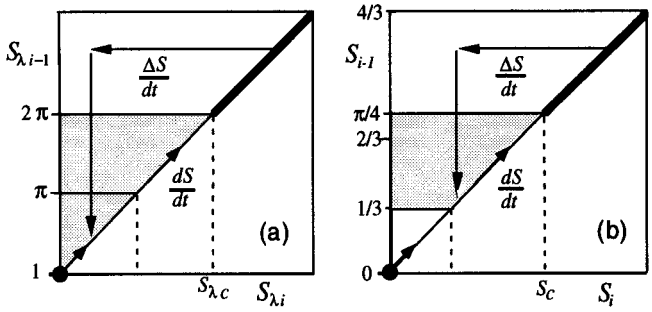

FIG. 9. SOC state-space dynamics. The attractor is shown as a shaded area. (a) River meandering. Sinuosity across one meander wavelength. (b) Grainpile, using the whole slope angle as the state parameter, measured in radians.

and active. In state space, this means that S_a is located within the basin of repulsion of $S_{\min}$. If instability (i) is stabilized, the dynamics of S_a will also die down. Assume such a frozen state and then introduce an infinitesimally small perturbation. If $2\pi \leqslant S_\lambda \leqslant 6\pi$, if a point of instability has appeared, and if the perturbation occurs exactly at this point, repulsion will occur. Hence this sinuosity region contains an unstable, fixed set. If $1 < S_\lambda < 2\pi$, an infinitesimally small perturbation will not cause any sudden change; hence this interval as a whole is a stable (attracting) fixed set. The span of the attracting region is the triangular space between the points (1,1), $(2\pi,2\pi)$, and $(1,2\pi)$ [Fig. 9(a)].

The simplest state parameter of a two-dimensional SOC grainpile is the angle between the apex and the edge of the pile. The critical, minimally stable angle is 45° (based on data in [3]). The pile will locally build above this angle due to instability (i), but these slopes are unstable, and deep, slide-type avalanches [instabilities (iii) and (iv)] bring the pile angle to the angle of sliding (approximately $\frac{2}{3}$ rad) or lower, depending of the momentum of the sliding mass. Any slope interval with S above this value is unstable to rupture or sliding of grain-locked domains and rolling of surface grains; hence all geometries represented in the set $S_a = \{S > 45°\}$ repel the macroscopic motion $\Delta S/dt$ [Fig. 9(b)].

In both the river and the grainpile, the $S_{\min}$ repeller of microscopic motion is caused directly by external forcing under a range of boundary conditions and is *independent* of any internal factors of the system. Also, avalanche motion is deflection of trajectories by a repelling point or set and requires the presence of the independent repeller. A state-space geometry occurs such that these two opposing repellers (one for each type of motion) have partially overlapping basins. This overlapping region encloses a strange attractor [21,22].

This attractor is a temporal projection of the complete spatiotemporal strange attractor of the system, which is the actual grainpile surface or river planform (the river stays within a bounded domain, the meander belt, without ever repeating or intersecting itself). If meandering is constrained by valley geometry, F_a may be prevented from arising, in which case fractal geometry does not emerge. Instead, self-organization reaches only a periodic symmetry and the attractor becomes a limit cycle [18].

VII. CONCLUSION

Emergence of the SOC state in any dynamical system requires three necessry conditions.

(i) The presence of two antagonistic forces, $F_d\uparrow$ and $F_a\downarrow$, such that $F_d\uparrow$ causes the motion dS/dt and $F_a\downarrow$ causes the motion $\Delta S/dt$.

(ii) A one-way contingency between the two forces, such that F_a is always contingent on F_d, but F_d is not contingent on F_a.

(iii) Both forces must act as repellers in state space, such that F_d repels dS/dt and F_a repels $\Delta S/dt$.

It follows from conditions (i) and (ii) that F_d is caused by external driving and F_a arises internally in the system. Condition (ii) means that F_a if, and only if, F_d. (F_a cannot act in the system unless F_d acts in the system.) Contingency implies dependence, but not necessarily a monotonic functional relationship $F_a=f(F_d)$. The contingency is one-way, because although F_d in most SOC systems will be influenced by F_a, it may well be entirely independent of F_a. The absence of contingency of F_d on F_a means that F_a does not have to be present for F_d to act indefinitely. [However, if F_a does not arise, the dynamics is no longer in the SOC state, and $S\rightarrow\infty$ [7]. Violation of SOC in the absence of F_a is stated as condition (i).] If the two forces were both independent of each other, they could still be in a balance to form a stationary state, but this steady state would not be robust (independent of initial conditions). To the contrary, it would require careful fine-tuning of parameters.

The physical meaning of condition (ii) is the same for both the two systems considered. Increase of S means that the mass of the system increases (the river is getting longer and the grainpile higher). Hence

$$F_d\uparrow=\frac{d\mathbf{p}}{dt}=\mathbf{v}_d\frac{dm}{dt},\quad \text{where}\quad \frac{dm}{dt}>0 \tag{24}$$

and $\mathbf{p}$ is the momentum of the whole system. The velocity of driving for the whole system, $\mathbf{v}_d$, is constant (given constant discharge of the river and a constant rate of addition of grains to the pile). Numerical simulations of river meandering under constant discharge have confirmed that the total rate of change due to F_d stays constant while local erosion rates vary from one point to another [7]. Each cutoff event of the river is caused directly by the meandering motion, and each grain avalanche directly by the addition of grains. Thus,

$$F_a\downarrow=\frac{\Delta\mathbf{p}}{dt}=\mathbf{v}_d\frac{\Delta m}{dt},\quad \text{where}\quad \frac{\Delta m}{dt}<0, \tag{25}$$

or

$$F_a\downarrow=F_d\uparrow\frac{\Delta m}{dm}=\frac{d\mathbf{p}}{dt}\frac{\Delta m}{dm},\quad \text{where}\quad \frac{\Delta m}{dm}<0 \tag{26}$$

in accordance with conditions (i) and (ii).

If the forces are acting as attractors instead of repellers, the dynamics will lead to a fractal basin boundary instead of an SOC strange attractor. However, more complex mixed cases will still lead to SOC. In these cases, each force acts as an attractor for one type of motion and a repeller for the other. Condition (iii) requires only that either force must have repelling action for different types of motion.

ACKNOWLEDGMENTS

I thank Alan Howard for the use of his meandering river simulator, and Gary Parker for a careful reading of Sec. III. Per Bak and Gary Stephens provided valuable comments.

[1] P. Bak, C. Tang, and K. Wiesenfeld, Phys. Rev. Lett. **59**, 381 (1987); M. Paczuski and P. Bak, Phys. Rev. E **48**, R3214 (1993); S. Maslov, M. Paczuski, and P. Bak, Phys. Rev. Lett. **73**, 2162 (1994); M. Paczuski, S. Maslov, and P. Bak, Phys. Rev. E **53**, 414 (1996).

[2] P. Bak and M. Creutz, in *Fractals in Science*, edited by A. Bunde and S. Havlin (Springer-Verlag, Berlin, 1994).

[3] V. Frette, K. Christensen, A. Malthe-Sørenssen, J. Feder, T. Jøssang, and P. Meakin, Nature (London) **379**, 49 (1996); J. J. Alonso and H. J. Herrmann, Phys. Rev. Lett. **76**, 4911 (1996); C. H. Scholz, *The Mechanics of Earthquakes and Faulting* (Cambridge University Press, Cambridge, 1990); K. Mogi, Tectonophysics **21**, 273 (1974); C. A. Coulomb, Acad. Sci. Paris Mem. Math. Phys. **7**, 343 (1776).

[4] H.-H. Stølum, Ph.D. thesis, Cambridge University, England, 1996.

[5] A. Thess, J. Sommeria, and B. Jüttner, Phys. Fluids **6**, 2417 (1994); B. Jüttner, A. Thess, and J. Sommeria, *ibid.* **7**, 2108 (1995); H. A. Einstein and H. W. Shen, J. Geophys. Res. **65**, 5239 (1964); H.-Y. Chang, D. B. Simons, and D. A. Woolhiser, J. Waterways, Harbors Coastal Eng. ASCE **97**, 155 (1971); C. R. Smith, in *Coherent Flow Structures in Open Channels*, edited by P. J. Ashworth *et al.* (Wiley, Chichester, 1996).

[6] G. Parker and E. D. Andrews, J. Fluid Mech. **162**, 139 (1986); K. Mahmood, M. I. Haque, and D. Budhu, in *Mechanics of Alluvial Channels*, edited by K. Mahmood, M. I. Haque, and A. M. Choudri (Water Resources, Littleton, CO, 1988).

[7] H.-H. Stølum, Science **271**, 1710 (1996).

[8] S. Ikeda, G. Parker, and K. Sawai, J. Fluid Mech. **112**, 363 (1981).

[9] J. E. Pizzuto and T. S. Meckelnburg, Water Resour. Res. **25**, 1005 (1989); K. Hasgawa, J. Hydraulic Eng. ASCE **115**, 744 (1989).

[10] H. Johannesson and G. Parker, J. Hydraulic Eng. ASCE **115**, 289 (1989); **115**, 1019 (1989); in *River Meandering*, edited by S. Ikeda and G. Parker, Water Resources Monograph No. 12 (American Geophysical Union, Washington, DC, 1989).

[11] H. Anwar, J. Hydraulic Eng. ASCE **112**, 657 (1986).

[12] T. Sun, P. Meakin, and T. Jøssang, Water Resour. Res. **32**, 2937 (1996).

[13] G. Parker and E. Andrews, J. Fluid Mech. **162**, 139 (1986).

[14] R. LeB Hooke, J. Geol. **83**, 543 (1975).

[15] H. Kikkawa, S. Ikeda, and A. Kitagawa, J. Hydraulic Eng. ASCE **102**, 1327 (1976); G. Parker, in *River Meandering*, edited by C. M. Elliott (ASCE, CITY, 1984).

[16] G. Parker, K. Sawai, and S. Ikeda, J. Fluid Mech. **115**, 303 (1982).

[17] J. Rosendahl, M. Vekic, and J. E. Routledge, Phys. Rev. Lett. **73**, 537 (1994); H. J. Feder and J. Feder, *ibid.* **66**, 2669 (1991).

[18] R. C. Hilborn, *Chaos and Nonlinear Dynamics* (Oxford University Press, New York, 1994); A. A. Tsonis, *Chaos* (Plenum, New York, 1992); H. G. Schuster, *Deterministic Chaos*, 2nd ed. (VCH, Weinheim, 1989).

[19] The actual fixed point is never reached in nature because it requires the flow velocity profile to be symmetric, i.e., flow must be entirely laminar. (The perfectly laminar state can be realized experimentally [20], but not in natural channels due to boundary roughness.)

[20] V. C. Patel and M. R. Head, J. Fluid Mech. **38**, 181 (1969).

[21] Originally suggested by P. Bak. The SOC attractor has been studied in detail by F.-J. Elmer, Phys. Rev. E **50**, 4470 (1994), and D. Chang, S.-C. Lee, and W.-J. Tzeng, *ibid.* **51**, 5515 (1995), for two one-dimensional models.

[22] A *strange attractor* is a fractal invariant set. It is a bounded region of state space in which the trajectory covers every point in the course of time without anywhere iterating a previous path. Since such a trajectory becomes infinitely long within a bounded domain it is fractal [18]. This is seen as a self-similar size distribution of the triangular shapes and clusters of triangular shapes caused by each avalanche (Fig. 3). The scaling distribution of simulated and actual river cutoff avalanches is demonstrated in [7,23] and scaling of experimental grainpile avalanches by Frette *et al.* [3].

[23] H.-H. Stølum and P. F. Friend, Earth Planet. Sci. Lett. (to be published).